

A cyclin-dependent kinase inhibitor inducing cancer cell differentiation: Biochemical identification using *Xenopus* egg extracts

(chemical libraries/cell cycle)

GUSTAVO R. ROSANIA*, JOHN MERLIE, JR.†, NATHANAEL GRAY*, YOUNG-TAE CHANG*, PETER G. SCHULTZ*‡, AND REBECCA HEALD†‡

*Department of Chemistry and Howard Hughes Medical Institute, and †Department of Molecular and Cell Biology, University of California, Berkeley, CA 94720

Contributed by Peter G. Schultz, March 1, 1999

ABSTRACT Cellular differentiation is a complex process involving growth arrest, exit from the cell cycle, and expression of differentiated cell-type-specific functions. To identify small molecules promoting this process, a chemical library was screened by using a myeloid leukemic cell line that retained the potential to differentiate in culture. In the presence of a purine derivative, aminopurvalanol (AP), cells acquired phenotypic characteristics of differentiated macrophages and became arrested in the cell cycle with a 4N DNA content. AP also inhibited mitosis in *Xenopus* egg extracts, suggesting that it acted on an evolutionarily conserved cell cycle regulatory pathway. Affinity chromatography and biochemical reconstitution experiments with *Xenopus* egg extracts identified cyclin-dependent kinase (CDK) 1–cyclin B as a target of the compound. Although AP potently inhibited immunoprecipitates of both human CDK1 and CDK2 from human leukemic cell extracts, our results indicate that the compound preferentially targets the G₂/M-phase transition *in vivo*.

To inhibit cancer cell proliferation, therapies have been developed by using natural inducers of cellular differentiation such as all-*trans*-retinoic acid (RA). Human leukemic cell lines that express phenotypic characteristics of differentiated cells in response to RA have served as model systems to study differentiation-inducing agents (1). Inside the cell, RA binds to a specific RA-receptor protein that modulates transcription, leading to growth arrest in the G₁ phase of the cell cycle and expression of differentiation markers (2). When used in combination with cytotoxic drugs, RA has been shown to induce remission in patients with acute promyelocytic leukemia (3). These observations have stimulated a search for other differentiation-promoting compounds, as possible therapeutic agents and as molecular probes of the cellular differentiation process.

Protein kinases constitute another potential target of differentiation-promoting compounds. The expression and activity of protein kinases regulating cell cycle progression, signal transduction, and gene expression can determine whether a cell differentiates or proliferates to become cancerous (4, 5). Selective kinase inhibitors were previously identified by screening chemical libraries of 2,6,9-substituted purine derivatives, using *in vitro* phosphorylation reactions with purified kinases (6, 7). Because purines with different substituents have shown specificity toward different kinases (7), we sought to determine whether any compound in the purine library could selectively influence the differentiation process. One purine derivative, aminopurvalanol (AP), was identified based on its

ability to promote the expression of differentiated characteristics in human leukemic cells. Using a biochemical depletion-reconstitution approach with extracts from *Xenopus* eggs, cyclin-dependent kinase (CDK) 1 was identified as a functional target of the compound.

MATERIALS AND METHODS

Chemicals and Reagents. All compounds were obtained from Sigma/Aldrich, unless otherwise indicated.

Cell Culture. Human U937 leukemic cells were obtained from the American Type Culture Collection. Cells were grown in RPMI 1640 medium plus 20% FCS. Cells were kept at 37°C in 5% CO₂/95% air.

Chemical Synthesis. Detailed procedures for AP, trimethyl-AP, and synthetic intermediates are described in the supplemental data published on the PNAS web site (www.pnas.org). P-Matrix was synthesized from commercially available 2-amino-6-chloropurine. 2-Amino-6-chloropurine was converted to 2-fluoro-6-chloro-9-isopropylpurine by using an aqueous fluoroboric acid diazotization procedure followed by a regioselective N-9 alkylation with 2-propanol under Mitsunobu conditions. The 6 position was then substituted with 4-amino-2-chlorobenzoic acid, followed by substitution at the 2 position with (*R*)-valinol. The resulting 2-(1*R*)-(isopropyl-2-hydroxyethylamino)-6-(3-chloro-4-carboxyanilino)-9-isopropylpurine was coupled to 1-*tert*-butyloxycarbonyl-1,8-diamino-3,6-dioxaoctane by using diisopropylcarbodiimide. The Boc group was removed with trifluoroacetic acid and the resulting primary amino group was coupled to carbonylimidazole-activated agarose (Reacti-GelR Pierce, product 20259). C-matrix was prepared identically except no amination is performed at the C-2 position.

Differentiation Assay. An in-house synthetic library of diverse 2,6,9-substituted purine derivatives was used for screening. Compounds in 10 mM DMSO stocks were diluted to 10 μM in cell growth medium. Approximately 2 × 10⁴ cells were seeded per well. DMSO (0.1%) was added to negative controls and 10 μM RA was added to positive controls. Cells were allowed to grow and differentiate for 4 days at 37°C in 5% CO₂/95% air.

Nitroblue Tetrazolium (NBT) Assay. To a 100-μl cell suspension, an equal volume of RPMI 1640 medium containing NBT at 1 mg/ml (Pierce) and 300 nM phorbol 12-myristate

Abbreviations: AP, aminopurvalanol; RA, all-*trans*-retinoic acid; CDK, cyclin-dependent kinase; NBT, nitroblue tetrazolium; TUNEL, terminal deoxynucleotidyltransferase-mediated UTP end labeling; PI, propidium iodide.

‡To whom reprint requests should be addressed: P.G.S. at the Department of Chemistry/Howard Hughes Medical Institute, University of California, Berkeley, CA 94720 or R.H. at the Department of Molecular and Cell Biology, University of California, Berkeley, CA 94720. e-mail: heald@socrates.berkeley.edu.

The publication costs of this article were defrayed in part by page charge payment. This article must therefore be hereby marked "advertisement" in accordance with 18 U.S.C. §1734 solely to indicate this fact.

PNAS is available online at www.pnas.org.

13-acetate was added to activate the cells, and cells were then incubated for 2.5 h at 37°C in 5% CO₂/95% air. The fraction of cells containing blue formazan deposits was determined with a microscope, using transmitted light illumination and ×200 magnification. Between 50 and 100 randomly selected cells were counted from each sample.

3-(4,5-Dimethylthiazol-2-yl)-2,5-diphenyl tetrazolium bromide (MTT) Assay. MTT (1 mg/ml) was added to the cell suspension and incubated for 2 h at 37°C in a 5% CO₂/95% air atmosphere. After the incubation period, the blue formazan product was solubilized as described (8). Absorbance was measured at 550 nm with an EAR400-AT plate reader (SLT Lab Instruments, Research Triangle Park, NC).

Apoptosis Assays. For terminal deoxynucleotidyltransferase-mediated UTP end labeling (TUNEL) assays, cells were washed with PBS, fixed in 4% paraformaldehyde in PBS, and permeabilized with 0.1% Triton X-100 in PBS. For labeling, cells were incubated with 50 μl of TUNEL reaction mixture (*in situ* cell death detection kit, fluorescein; Boehringer Mannheim) plus 5 μl of RNase A at 3 mg/ml (Boehringer Mannheim), at 37°C for 1.5 h. At that time, 1 ml of propidium iodide (PI; Molecular Probes) at 0.04 mg/ml in PBS was added, and the cells were analyzed by flow cytometry. For assaying DNA fragmentation patterns, cells were harvested and resuspended in 10 mM Tris-HCl, pH 7.5/10 mM EDTA/0.1% Triton X-100 for 1 h. Debris was removed by centrifugation. Fragmented DNA in supernatant was precipitated with 2.5 vol of EtOH and 0.5 vol 7.5 M ammonium acetate overnight at -20°C. DNA was spun down, washed two times with 80% EtOH, and resuspended in TE buffer containing RNase A at 20 μg/ml for 30 min at 37°C. DNA was electrophoresed on 1.8% agarose gel and visualized with ethidium bromide under UV illumination.

CD11b Staining. To assay for expression of CD11b, 5×10^5 cells were suspended in 100 μl of PBS containing 150 nM phorbol 12-myristate 13-acetate, 1% BSA, and 10 μl of FITC-labeled anti-CD11b monoclonal antibody, at 37°C for 45 min. After fixing with 1.5 ml of 2% paraformaldehyde in PBS for 20 min, cells were permeabilized with 0.1% Triton X-100 in PBS for 20 min. After permeabilization, cells were incubated in a solution of RNase A at 0.5 mg/ml in PBS at 37°C for 30 min. Cells were resuspended in PI at 0.04 mg/ml in PBS and analyzed by flow cytometry.

Flow Cytometry and Cell Cycle Analysis. FITC- and PI-stained cells were analyzed by using a Coulter instrument. For each experiment, more than 50,000 cells were analyzed. Cell cycle distributions were calculated with the MULTICYCLE program (Phoenix Flow Systems, San Diego). After flow cytometric analysis, PI-stained cells were observed with a rhodamine filter set, on a Zeiss Axioskop microscope using ×1,000 magnification. In each sample, at least 100 randomly-selected cells were counted for the presence of cells with condensed chromosomes to determine the fraction of cells in mitosis.

Xenopus Egg Extracts. We prepared cytosolic factor-arrested extracts (CSF) as detailed (9) with the exceptions that cytochalasin D was used in place of cytochalasin B and a versilube overlay was not used during the crushing spin. For high-speed extract, fresh CSF extract was spun at 150,000 × *g* in a TLA-100.3 ultracentrifuge rotor (Beckman) for 30 min at 4°C.

Spindle Assay. Spindle assembly assays were performed as described (10). For addition experiments, AP, demembrated sperm nuclei, and rhodamine-labeled tubulin were added to fresh extracts and incubated for 45 min at 20°C. For matrix-treatment experiments, fresh extracts were incubated with either active or control matrices for 30 min at 4°C. After spinning out matrices, recovered extracts were incubated with sperm nuclei and rhodamine-labeled tubulin for 45 min at 20°C. For rescue experiments, pure CDK1-cyclin B obtained from H. Wilhelm (11) with an activity of 93 pmol per min per μl was added at 0.1 vol to matrix-treated extract.

Spindle assembly was assayed by spinning extracts onto coverslips (10) except that centrifugation was done at 10,000 rpm in an HB-6 rotor (Sorvall) for 12 min at 16°C. After fixation in -20°C methanol, coverslips were washed once with PBS/Nonidet P-40, stained with Hoechst 38258 to visualize DNA, and washed four times with PBS/Nonidet P-40. After mounting on glass slides, coverslips were analyzed and imaged with a Nikon Eclipse E600 microscope and a cooled charge-coupled device camera (Technical Instruments, San Francisco).

Histone H1 Kinase Assays. Histone H1 kinase assays were based on published methods (12) except that EB buffer was prepared without PMSF. Extract was diluted 1:20 in EB, flash-frozen, and stored at -80°C. Kinase activity was assayed by incubating 5 μl of sample with 5 μl of assay mixture: 0.75 × EB with histone H1 (Boehringer Mannheim) at 2 mg/ml, 0.6 mM ATP, and [γ -³²P]ATP (Amersham) at 0.1 μCi/μl (1 Ci = 37 GBq). Incubations ran for 15 min at which time 6 μl of each incubation was blotted onto squares of P81 phosphocellulose paper (Whatman). Squares were then washed three times with 150 mM H₃PO₄, washed once with EtOH, dried, and loaded into scintillation vials with scintillation fluid. Radioactivity was measured on the ³²P cycle in an LSC scintillation counter (Beckman).

DNA Replication Assays. Linearized plasmid DNA (0.3 μg) immobilized on magnetic beads (Dyna) was incubated in 30 μl of interphase extract at 20°C for 2 h in the presence of 5 μCi of [³²P]dCTP (13), and 200 or 300 μM AP, aphidicolin at 50 μg/ml, or 0.01 vol of DMSO was added at the beginning of the reaction. Beads were retrieved on magnets, washed extensively with 10 mM Hepes, pH 7.6/3 mM MgCl₂/0.5 mM EGTA/0.05% Triton X-100, then transferred to scintillation vials containing scintillation fluid. Radioactivity was measured on the ³²P cycle in an LSC.

Gel and Immunoblot Analysis. High-speed extract samples were analyzed by silver stain or immunoblot and resolved on a 10% SDS/polyacrylamide gel. Crude extract protein samples analyzed by immunoblot were resolved on 12% SDS/polyacrylamide gels, transferred to nitrocellulose (Schleicher & Schuell), and processed for ECL (Amersham). CDK1 was detected with a mouse monoclonal antibody (clone A17.1.1, Calbiochem) raised against *Xenopus* CDK1. CDK2 was detected with a rabbit polyclonal antibody (Daniel Donoghue, Univ. of California, San Diego) raised against *Xenopus* CDK2.

CDK Immunoprecipitation. For CDK2 immunoprecipitation, 1.5×10^8 U937 cells were grown in proliferation medium to a concentration of 5×10^5 cells per ml. For CDK1 immunoprecipitation, the cell population was synchronized in mitosis with 1 μM Taxol for 16 h. All procedures were carried out at 4°C. Cells were harvested, resuspended in an equal volume of EB, and homogenized by using a syringe, with 15 strokes through a 26.5-gauge needle. After homogenization, another volume of EB plus 1% Triton X-100 was added to the cell suspension and left to incubate for 30 min. Nuclei and debris were then removed by centrifugation. Supernatant was transferred into a different tube and incubated with 50 μl of anti-CDK2 (M2)-G (Santa Cruz Biotechnology) or 50 μl of anti-CDC2 p34 (17) -agarose conjugate (Santa Cruz Biotechnology) for 1 h with continuous agitation. The matrix was then washed with EB, and CDK1 or CDK2 activity was monitored by using histone H1 kinase assays.

RESULTS

U937 cells (14, 15) were used to screen for purine derivatives affecting cellular differentiation. Initially, 150 diverse compounds (6) were assayed for their ability to induce the expression of NBT-reducing activity, a characteristic of differentiated macrophages and neutrophils. Only one compound in the library, AP (Fig. 1), consistently induced NBT-reducing activ-

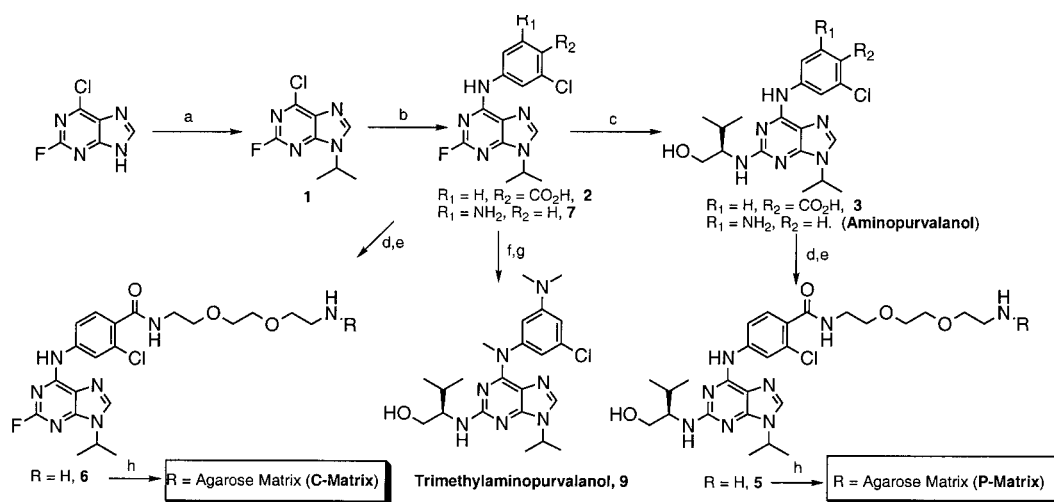


FIG. 1. Synthesis of AP, trimethyl-AP, P-matrix, and C-matrix. Conditions: (a) 2.0 equivalents of triphenylphosphine, 2.0 equivalents of diethylazodicarboxylate (DEAD), 2.0 equivalents of 2-propanol, tetrahydrofuran (THF). (b) 1.0 equivalent of 4-amino-2-chlorobenzoic acid or 5-chloro-1,3-phenylenediamine, 3.0 equivalents of diisopropylethylamine (DIEA), *n*-butanol, 90°C, 12 h. (c) 5.0 equivalents of (*R*)-(-)-2-amino-3-methyl-1-butanol, 5.0 equivalents of DIEA, *n*-butanol, 110°C, 18 h. (d) 1.05 equivalents of 1,3-diisopropylcarbodiimide (DIC), 1.05 equivalents of hydroxybenzotriazole, 2.0 equivalents of DIEA, 2.0 equivalents of 1-*tert*-butyloxycarbonyl-1,8-diamino-3,6-dioxaoctane (**4**), 0.05 equivalents of 4-dimethylaminopyridine, dimethylformamide (DMF)/CH₂Cl₂/1,4-dioxane, 1:1:1 (vol/vol). (e) Trifluoroacetic acid/CH₂Cl₂/H₂O/(CH₃)₂S, 45:45:1:1 (vol/vol), 12 h. (f) 17.3 equivalents of NaH, 10.7 equivalents of methyl iodide, DMF, 12 h. (g) 33.0 equivalents of (*R*)-(-)-2-amino-3-methyl-1-butanol, *n*-butanol, 140°C, 12 h. (h) 45.0 mM compound **5** or **6**, 1.5 ml of ReactiGel 6X (Pierce, product 20259), 0.1 M aqueous K₂CO₃, 12 h.

ity in U937 cells to levels similar to those induced by retinoic acid (Fig. 2A). To characterize the biological activity of AP, its effects on the cellular differentiation process were examined in greater detail.

Dose-response analysis revealed that AP acted in two ways to promote the differentiated phenotype: by inducing expression of NBT-reducing activity (Fig. 2A and C) and by inhibiting growth of undifferentiated cells (Fig. 2B). At 5 μ M, the compound decreased the viability of proliferating U937 cells by 26% ($P < 0.001$, $n = 4$, *t* test), but it affected the viability of RA-differentiated U937 cells by only 6% ($P = 0.02$, $n = 5$; *t* test). At higher concentrations, AP was cytotoxic, decreasing the number of cells at the end of the experiment. These results indicated that AP acted both directly and indirectly to promote growth of cells with the differentiated phenotype.

AP also induced the expression of the CD11b integrin, another differentiation marker. Flow cytometry analysis of cells costained with FITC-conjugated anti-CD11b antibodies and PI was used to quantify the level of CD11b expression and DNA content, respectively. Untreated samples displayed a range of DNA contents characteristic of proliferating cell populations, and few cells stained positive for CD11b (Fig. 2D). In contrast, 5 μ M AP increased the fraction of cells with a 4N DNA content, and the majority of these cells stained positive for CD11b (Fig. 2E). AP also induced cellular fragmentation indicative of cell death. To determine whether the effects of AP were specific to the drug, an N-methylated derivative of AP (trimethyl-AP; Fig. 1) was subjected to the same assays. Trimethyl-AP did not increase the fraction of cells expressing CD11b nor did it cause a change in the range of the DNA distribution in the cell population (Fig. 2F).

AP inhibited cell growth primarily by arresting the cells in the G₂ phase of the cell cycle and, at higher concentration, triggered apoptosis. The presence of apoptotic nuclei in AP-treated cells was determined in conjunction with the cellular DNA content using flow cytometry. DNA was stained with PI, and apoptotic nuclei were detected with the TUNEL assay, in which fluorescent nucleotides are enzymatically incorporated onto the ends of DNA fragments resulting from the apoptotic

process (16). In these experiments, 5 μ M AP increased the number of cells with a 4N DNA content as early as 8 h after the beginning of treatment (Fig. 3A and B). Under the same conditions, doses higher than 10 μ M led to cellular fragmentation and cells with an irregular DNA distribution, characteristic of apoptotic cell populations (Fig. 3C). These observations were supported by the results obtained with the TUNEL assay (Fig. 3D-F), indicating that apoptosis was not directly induced by the drug at doses that promoted cellular differentiation.

In dose-response and time course experiments, AP treatment caused a progressive increase in the G₂/M-phase fraction with a concomitant decrease in the G₁-phase fraction (Fig. 3G and H). The S-phase fraction remained relatively constant during the course of the experiment, indicating that the G₁/S and S/G₂ transitions proceeded normally in the presence of the drug, at concentrations that promoted cellular differentiation. To distinguish between a block in G₂ and M phase, cells stained with PI were scored morphologically by fluorescence microscopy for the presence of condensed chromosomes characteristic of mitotic cells. In control cells, 5% of the population was in mitosis, whereas in the AP-treated cells, less than 1% of the population was in mitosis (values $\pm 1\%$; $n = 3$), indicating that AP induces a specific G₂-phase block.

The cell cycle arrest induced by AP raised the possibility that the compound interfered with the function of CDK1, which regulates entry into mitosis. In animal cells, S phase is induced by CDK2 complexed with S-phase cyclins (E and A types), and M phase is induced by CDK1 complexed with M-phase cyclins (A and B types) (17). To identify the molecular mechanism behind AP action, we performed experiments with *Xenopus* egg extracts. In addition to providing a biochemically tractable system, *Xenopus* egg extracts can progress through both interphase and mitotic cell cycle states in which many cellular processes such as DNA replication and mitotic spindle assembly are faithfully executed *in vitro* (18, 19). Because the biochemical machinery regulating cell cycle progression is highly conserved from yeast to human (20), we reasoned that *Xenopus* egg extracts could be used to investigate in more

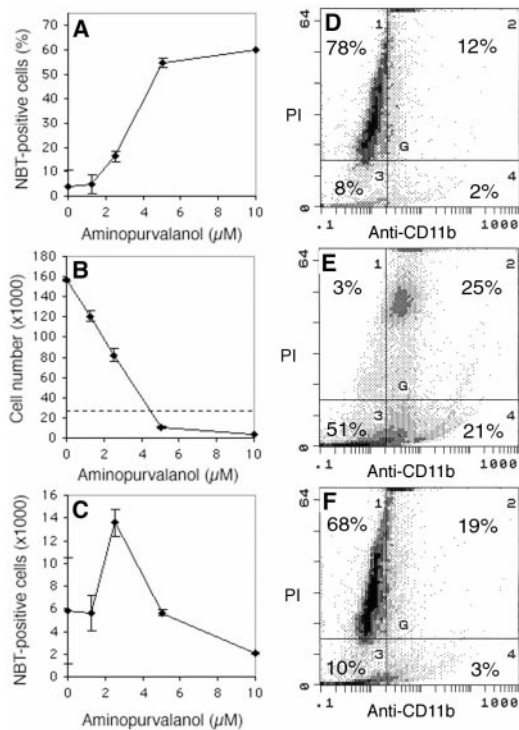


Fig. 2. Effect of AP on U937 cell differentiation. (A–C) Dose-response analysis. Cell counts were determined with the use of a hemocytometer. Each data point is the average of at least three experiments. (A) The fraction of NBT-positive cells increases with increasing concentrations of the drug. (B) The number of viable cells remaining after treatment with AP decreases with increasing concentrations of the drug. The dashed line indicates the starting number of cells. (C) The absolute number of cells expressing NBT-reducing activity after treatment with the drug is maximal between 2.5 and 5 μ M AP. (D–F) Bivariate plots of cells stained for DNA content with PI and CD11b expression with an FITC-conjugated anti-CD11b monoclonal antibody and analyzed by flow cytometry. Numbers indicate the fraction of the total number of events in each quadrant. (D) Untreated cells display a range of DNA content typical of unsynchronized cells and few possess the CD11b antigen. (E) Cells treated with 5 μ M AP show an accumulation of CD11b-positive cells with a 4N DNA (quadrant 2). Note the presence of cells with subdiploid DNA content (quadrants 3 and 4). (F) Cells treated with a closely related AP analogue look similar to the untreated population with little cellular fragmentation and few of the cells express CD11b antigen.

detail the AP-induced cell cycle defects and identify targets of AP action.

AP inhibited mitosis when added to *Xenopus* egg extracts (18). In control reactions, *Xenopus* sperm nuclei nucleated polarized microtubule arrays around condensed chromosomes, forming “half spindles” that fused pair-wise to form bipolar spindles (Fig. 4A). In contrast, reactions treated with 200 μ M AP were characterized by partially decondensed sperm nuclei and extensive long microtubules characteristic of interphase extracts (Fig. 4B). Histone H1 kinase activity, used as a measure of CDK1 activity, was reduced to interphasic levels in AP-treated extracts. The effects of the compound appeared to be dose dependent. In the presence of 100 μ M AP, kinase activity was reduced to an intermediate level. Although spindles did not form, some microtubule organization was apparent as large disorganized astral arrays. At 40 μ M AP, mitotic spindle structures formed with less severe effects on morphology and histone H1 kinase activity (data not shown).

To identify the molecular target of AP, an affinity matrix was constructed by using a close structural analogue of AP bearing a *para*-carboxyl group attached via a short linker to an agarose-based solid support (P-matrix; Fig. 1). As a negative

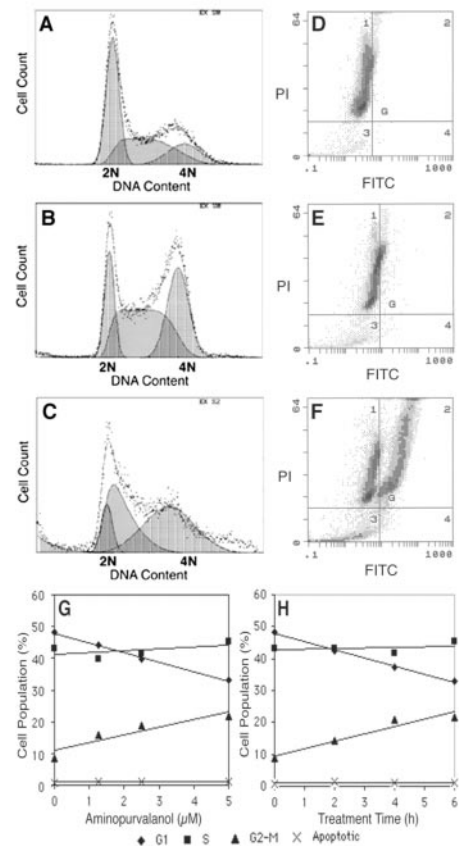


Fig. 3. Cell cycle changes induced by AP, as assayed by flow cytometry. For all the experiments, DNA content was determined for each cell based on the amount of PI labeling. DNA fragmentation was simultaneously detected by FITC-labeled nucleotide incorporation onto free DNA ends, using the TUNEL reaction. (A–C) Scattered data points represent actual number of cells with various contents of DNA. (A) Untreated, proliferating cell population. (B) Cell population treated with 5 μ M AP for 8 h. (C) Cell population treated with 40 μ M AP for 8 h. The curves shaded gray represent an estimated number of cells with a 2N, 4N, and intermediate DNA content, as calculated with the MULTICYCLE program. (D–F) TUNEL assay results from an untreated cell population (D), a cell population treated with 5 μ M AP for 8 h (E), and a population treated with 40 μ M AP for 8 h (F). Note the presence of a prominent FITC-labeled cell population on the upper right quadrant and the increased population of fragmented cells in lower left quadrant. (G) Concentration-dependent changes in the G₁-, S-, and G₂/M-phase cells in cell populations treated with AP for 6 h, as determined from the distribution of DNA per cell in the cell population. (H) Time-dependent changes in G₁-, S-, and G₂/M-phase populations treated with 5 μ M AP.

control, a matrix was prepared with an inactive derivative of AP containing a fluorine at the 2 position of the purine ring (C-matrix; Fig. 1). C-matrix treatment had no effect on mitotic spindle assembly or histone H1 kinase activity in extracts (Fig. 4C), whereas P-matrix inhibited mitosis and histone H1 kinase activity in a dose-dependent fashion, similar to the free compound (Fig. 4D). To identify the cellular targets of the active compound, proteins bound specifically to P-matrix were characterized. SDS/PAGE analysis of proteins eluted from P-matrix and C-matrix revealed a number of proteins bound to both matrices, but with one protein of about 34 kDa specifically bound to the P-matrix (Fig. 5A). Western blot analysis identified this P-matrix-specific band as CDK1 (Fig. 5B). Pretreatment of extracts with AP significantly reduced the amount CDK1 bound to P-matrix, indicating that the free compound could compete with P-matrix for CDK1 binding (Fig. 5D). These results suggested that AP interacts with and inhibits CDK1 activity, resulting in mitotic inhibition.

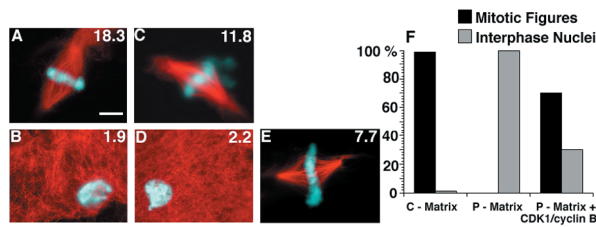


FIG. 4. Effects of AP and compound matrix treatment on spindle assembly reactions in *Xenopus* egg extracts and reconstitution experiment. (Bar = 10 μ m.) The measured histone H1 kinase activity in pmol per min per μ l for each reaction is shown in the upper right corner of each part. (A) Control reaction containing demembrated sperm nuclei yields bipolar spindles and high histone H1 kinase activity characteristic of mitotic extracts. (B) In the presence of 200 μ M AP, 100% of sperm nuclei decondense and microtubules grow long, with low histone H1 kinase activity characteristic of interphase extracts. (C) Extract treated with C-matrix still yields bipolar spindles and normal kinase activity levels. (D) Extract treated with P-matrix causes interphasic morphology and histone H1 kinase activity similar to treatment with the free compound. (E) Extract treated with P-matrix is rescued by the addition of pure CDK1–cyclin B, yielding bipolar spindles and higher histone H1 kinase activity. (F) Quantification of a representative rescue experiment. One hundred nuclei were counted for each condition. C-matrix treatment yielded nearly 100% mitotic figures, whereas P-matrix treatment resulted in 100% interphase nuclei. Addition of pure CDK1–cyclin B kinase (0.1 vol of 93 pmol per min per μ l) to P-matrix-treated extract resulted in 70% of the sperm nuclei forming mitotic figures.

Unexpectedly, a significant amount of CDK1 remained in P-matrix-treated extracts, indicating that not all of the CDK1 was bound by the P-matrix (Fig. 5B). However, the remaining

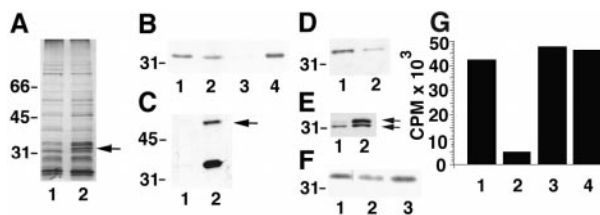


FIG. 5. Biochemical characterization of proteins bound to chemical compound matrices and effects of the compound on DNA replication. (A) Silver-stained gel of proteins eluted from C-matrix (lane 1) and P-matrix (lane 2). The arrow marks a band at 34 kDa specific for P-matrix. (B) Western blot analysis of 1 μ l of total extract treated with C-matrix (lane 1) or P-matrix (lane 2). Proteins eluted from C-matrix (lane 3) and P-matrix (lane 4) are equivalent to proteins retrieved from 10 μ l of extract. The blot is probed with anti-CDK1 antibodies and shows that CDK1 is found on P-matrix but not C-matrix, resulting in a partial depletion of CDK1 from P-matrix-treated extracts. (C) Western blot of C-matrix (lane 1) and P-matrix (lane 2) probed with both anti-CDK1 and anti-*Xenopus* cyclin B antibodies. The arrow indicates cyclin B, which is present only on P-matrix. (D) Western blot of proteins eluted from P-matrix incubated in extracts in the presence of DMSO (lane 1) or 100 μ M AP (lane 2) and probed with anti-CDK1 antibodies. Less CDK1 binds to the matrix in the presence of the free compound. (E) Western blot of proteins eluted from C-matrix (lane 1) and P-matrix (lane 2) probed with both anti-CDK1 and anti-CDK2 antibodies. A small amount of CDK2 binds to both matrices, whereas CDK1 binding is specific for P-matrix. Upper arrow, CDK1 at 34 kDa; lower arrow, CDK2 at 32 kDa. (F) Western blot probed with anti-CDK1 antibodies showing the amount of CDK1 remaining in C-matrix-treated extracts (lane 1), P-matrix-treated extracts (lane 2), and P-matrix-treated extracts that have been rescued by the addition of pure CDK1–cyclin B (lane 3). Addition of pure kinase restores CDK1 to normal levels. (G) DNA replication experiment showing that similar amounts of [³²P]dCTP are incorporated into immobilized plasmid DNA in interphase extracts in control reactions (1) and reactions containing 200 μ M (3) or 300 μ M (4) AP. Incorporation is inhibited by aphidicolin at 50 μ g/ml, a specific inhibitor of DNA replication (2).

CDK1 was not active as assayed by histone H1 kinase activity, indicating that it was in a state devoid of catalytic activity. Because mitotic CDK1 activation requires association with cyclin B, which is less abundant than CDK1 in *Xenopus* egg cytoplasm (19), we assayed cyclin B levels by Western blot analysis. Cyclin B was also found to be associated with P-matrix but not C-matrix but was not completely depleted from extracts by P-matrix treatment (Fig. 5C and data not shown). These results indicate that P-matrix binds active CDK1–cyclin B complexes. Because P-matrix can bind CDK1 in interphase extracts lacking cyclin B (data not shown), the association of the kinase complex appears to be through the purine-binding catalytic CDK1 subunit.

To probe whether P-matrix depletion was specific for CDK1 and M-phase induction, C- and P-matrices were analyzed on Western blots with anti-CDK2 antibodies. Similar amounts of CDK2 bound to both C- and P-matrices, indicating that AP interaction with CDK2 was less specific than with CDK1 (Fig. 5E). To determine whether AP interfered with S-phase progression by binding CDK2, DNA replication was measured in interphase extracts containing the compound (Fig. 5G). [³²P]dCTP was incorporated into immobilized plasmid DNA in the presence of up to 300 μ M AP but was inhibited by aphidicolin at 50 μ g/ml. Therefore, although AP bound to some CDK2 in the extract, it did not have a significant effect on the physiological activity of CDK2 in promoting S-phase progression. This result is consistent with the effects of the compound on U937 cells, which results in G₂- but not G₁- or S-phase arrest.

To test whether CDK1–cyclin B was the only activity required for mitotic progression removed from the extract by P-matrix, purified *Xenopus* CDK1–cyclin B was added back to the depleted extract. CDK1–cyclin B was prepared by adding cyclin B–glutathione S-transferase (GST) to *Xenopus* extracts and retrieving CDK1–cyclin B–GST on glutathione-agarose beads. The complex was further purified by mono S chromatography (11). In either an interphasic extract or a P-matrix-treated extract, approximately 70% of added sperm nuclei formed spindle arrays 45 min after addition of CDK1–cyclin B (Fig. 4E). Western blot analysis indicated that CDK1 protein was restored to levels found in C-matrix-treated extracts (Fig. 5F). Therefore, CDK1–cyclin B addition rescued spindle assembly and chromosome condensation in P-matrix-depleted extracts. This result is consistent with experiments showing that CDK1–cyclin B controls the passage of the cell cycle from G₂ phase into mitosis (18, 19), indicating that AP binds and inactivates CDK1 in *Xenopus* egg extracts.

To determine whether CDK1 was also a target of AP in human cells, the compound was tested in histone H1 kinase assays using CDK1 and CDK2 immunoprecipitates from U937 cell extracts. In these assays, AP potentially inhibited the activity of CDK1 (IC₅₀ = 196 \pm 31 nM) and CDK2 (IC₅₀ = 28 \pm 14 nM). To test whether AP inhibited CDK1 or CDK2 activity *in vivo*, the activity of both kinases was assayed in immunoprecipitates of U937 cell extracts obtained after treating proliferating cell populations with 5 μ M AP for 1 h. Compared with untreated cell populations, the compound inhibited the *in vivo* activity of CDK1 and CDK2 by 43% (SEM = \pm 13%, n = 5) and 66% (SEM = \pm 8%, n = 5), respectively. Therefore, AP inhibits CDK1 and CDK2 activity in U937 cells both *in vivo* and *in vitro*, with a greater potency toward CDK2. However, because AP preferentially inhibits G₂- to M-phase progression, the activity of CDK1–cyclin B appears to be the primary functional target of AP.

DISCUSSION

We have identified a unique CDK1/CDK2 inhibitor, AP, that promotes the expression of phenotypic markers characteristic of RA-differentiated U937 cells. Whereas RA induces U937

cell cycle arrest predominantly in G₁ phase, AP causes cell cycle arrest in G₂ phase, indicating that certain aspects of the differentiation process can be uncoupled from the stage at which cells exit the cell cycle and from the cellular DNA content. Although AP could block mitosis by inhibiting CDK1 directly, our results cannot exclude a role for CDK2 inhibition in the mechanism of G₂ arrest, especially since CDK2 is active during G₂ and may help activate CDK1 (21, 22). Consistent with a direct role for CDK inhibition in promoting expression of the differentiated phenotype, ectopic expression of the CDK inhibitors p21 or p27 in U937 cells also results in the acquisition differentiated phenotypes and arrest in the G₁ or G₂ phase of the cell cycle (23).

To identify the target of AP action, we used *Xenopus* egg extracts, a biochemically tractable system that retains the ability to progress through the entire cell cycle *in vitro*. The effect of the drug to block extracts in interphase was consistent with the G₂-phase cell cycle arrest in U937 cells. However, much higher concentrations of the drug were required in extracts. General differences in the potency of pharmacological inhibitors in *Xenopus* egg extracts vs. cells in culture are common and can be ascribed to the partitioning of the compounds into the protein and lipid phase of the extract, decreasing the effective concentration of free compound in solution. Nevertheless, we could demonstrate the specificity of the compound in this system by reconstituting affinity-matrix-treated extracts by addition of purified CDK1-cyclin B. Because *Xenopus* egg extracts can be modified to assay other cell cycle transitions (24), this biochemical depletion-reconstitution strategy can be used to identify the cellular targets of other small molecules affecting cellular differentiation and cell cycle progression.

The potent inhibition of U937 CDK1 and CDK2 immunoprecipitates by AP suggests that the activity of these kinases can influence the cellular differentiation process. Unlike the response of other mammalian cell lines to small molecule CDK inhibitors (25), U937 cells respond to low doses of AP by arresting in the cell cycle without undergoing apoptosis. This inhibition of cell growth might lead to the expression of differentiated characteristics by slowing down the cell cycle and thereby increasing the probability that a cell will take an alternative developmental pathway. Alternatively, inhibiting CDK1/CDK2 activity could directly affect transcriptional activity, leading to changes in gene expression patterns that alter the balance between proliferation and expression of the differentiated phenotype (26, 27). These two mechanisms are not mutually exclusive, and both may contribute to the manifestation of differentiated phenotypic characteristics of U937 cells treated with AP.

In cells and extracts, AP treatment causes arrest in the G₂ phase of the cell cycle without a major effect on the G₁/S phase. One explanation could be that G₁/S-phase progression is quantitatively less sensitive to CDK2 inhibition than G₂/M-phase progression is to CDK1 inhibition (28). Alternatively, the transformed phenotype of U937 cells could result in specific changes in cell cycle regulation. As many other cell lines originating from human tumors, U937 human leukemic cells express different cyclins in an unscheduled fashion (29, 30). Thus, we propose that abnormalities in the biochemical mechanism governing cell cycle progression in cancer cells could account for differences in the levels of CDK inhibition required to arrest cells at the G₁/S or G₂/M-phase transitions.

To conclude, the expression of differentiated characteristics in U937 cells treated with AP indicates that small molecule

CDK inhibitors can be used to alter the balance between cell growth and differentiation in cancer cells. The ability of AP to induce CD11b expression and NBT-reducing activity in human leukemic cells suggests that the effect of CDK inhibition goes beyond the cell cycle. AP should be useful for elucidating the role of CDK activity in the regulation of cell cycle progression and gene expression, in normal and transformed cells.

We thank H. Wilhelm (European Molecular Biology Laboratory, Heidelberg) for pure CDK1-cyclin B and anti-cyclin B monoclonal antibodies and Dr. Daniel Donoghue for anti-CDK2 antibodies. Y.T.C. acknowledges the financial support of the Korea Research Foundation made in the program year 1997.

- Breitman, T., Selonick, D. & Collins, S. (1980) *Proc. Natl. Acad. Sci. USA* **77**, 2936–2940.
- Love, J. M. & Gudas, L. J. (1994) *Curr. Opin. Cell Biol.* **6**, 825–831.
- Tallman, M. S., Andersen, J. W., Schiffer, C. A., Appelbaum, F. R., Feusner, J. H., Ogden, A., Shepherd, L., Willman, C., Bloomfield, C. D., Rowe, J. M. & Wiernick, P. H. (1997) *N. Engl. J. Med.* **337**, 1021–1028.
- Baghdassarian, N. & French, M. (1996) *Hematol. Cell Ther.* **38**, 313–323.
- Johnson, G. L. & Vaillancourt, R. R. (1994) *Curr. Opin. Cell Biol.* **6**, 230–238.
- Meijer, L. & Kim, S. H. (1997) *Methods Enzymol.* **283**, 113–128.
- Gray, N. S., Wodicka, L., Thunnissen, A.-M., Norman, T. C., Kwon, S., Espinoza, F. H., Morgan, D. O., Barnes, G., LeClerc, S., Meijer, L., *et al.* (1998) *Science* **281**, 533–538.
- Hansen, M. B., Nielsen, S. E. & Berg, K. (1989) *J. Immunol. Methods* **119**, 203–210.
- Murray, A. W. (1991) *Methods Cell Biol.* **36**, 581–605.
- Sawin, K. E. & Mitchison, T. J. (1991) *J. Cell Biol.* **112**, 925–933.
- Wilhelm, H., Anderson, S. S. L. & Karsenti, E. (1997) *Methods Enzymol.* **283**, 12–28.
- Felix, M. A., Pines, J., Hunt, T. & Karsenti, E. (1989) *EMBO J.* **8**, 3059–3069.
- Heald, R., Tournebize, R., Blank, T., Sandaltzopoulos, R., Becker, P., Hyman, A. & Karsenti, E. (1996) *Nature (London)* **382**, 420–425.
- Sundstrom, C. & Nilsson, K. (1976) *Int. J. Cancer* **17**, 565–577.
- Harris, P. & Ralph, P. (1985) *J. Leukocyte Biol.* **37**, 407–422.
- Gorczyca, W., Bruno, S., Yi, P.-N. & Darzynkiewicz, Z. (1993) *Cancer Res.* **52**, 1945–1955.
- Nigg, E. A. (1995) *Bioessays* **17**, 471–480.
- Murray, A. W. & Kirschner, M. W. (1989) *Nature (London)* **339**, 275–280.
- Murray, A. W., Solomon, M. J. & Kirschner, M. W. (1989) *Nature (London)* **339**, 280–286.
- Lew, D. J., Dulic, V. & Reed, S. I. (1991) *Cell* **66**, 1197–1206.
- Guadagno, T. M. & Newport, J. (1996) *Cell* **84**, 73–82.
- Rosenblatt, J., Gu, Y. & Morgan, D. O. (1992) *Proc. Natl. Acad. Sci. USA* **89**, 2824–2828.
- Liu, M., Lee, M. H., Cohen, M., Bommakanti, M. & Freedman, L. P. (1996) *Genes Dev.* **10**, 142–153.
- Smythe, C. & Newport, J. (1992) *Methods Cell Biol.* **35**, 449–468.
- Schutte, B., Nieland, L., van Engeland, M., Henfling, M. E. R., Meijer, L. & Ramaekers, F. C. (1997) *Exp. Cell Res.* **236**, 4–15.
- Robles, S. J., Shiyonov, P., Aristodemo, G. T., Raychaudhuri, P. & Adami, G. R. (1998) *DNA Cell Biol.* **17**, 9–18.
- Sidle, A., Palaty, C., Dirks, P., Wiggan, O., Kiess, M., Gill, R., Wong, A. K. & Hamel, P. A. (1996) *Crit. Rev. Biochem. Mol. Biol.* **31**, 237–271.
- Stern, B. & Nurse, P. (1996) *Trends Genet.* **12**, 345–350.
- Gong, J., Ardelt, B., Traganos, F. & Darzynkiewicz, Z. (1994) *Cancer Res.* **54**, 4285–4288.
- Hunter, T. & Pines, J. (1994) *Cell* **79**, 573–582.